

Data-Enabled Predictive Control for Fast Charging of Lithium-Ion Batteries with Constraint Handling

Kaixiang Zhang^{a,*}, Kaian Chen^{a,*}, Xinfan Lin^b, Yusheng Zheng^c, Xunyun Yin^d, Xiaosong Hu^c, Ziyou Song^e, Zhaojian Li^{a,**}

^aDepartment of Mechanical Engineering, Michigan State University, East Lansing, 48824, MI, USA.

^bDepartment of Mechanical and Aerospace Engineering, University of California Davis, Davis, 95616, CA, USA.

^cDepartment of Mechanical and Vehicle Engineering, Chongqing University, Chongqing, 400044, China

^dSchool of Chemical and Biomedical Engineering, Nanyang Technological University, 637459, Singapore

^eDepartment of Mechanical Engineering, National University of Singapore, 117575, Singapore

Abstract

Fast charging of lithium-ion batteries has gained extensive research interest, but most of the existing methods are either based on simple rule-based charging profiles or require explicit battery models that are non-trivial to identify accurately. In this paper, instead of relying on parametric battery models that are costly to derive and calibrate, we employ a novel data-enabled predictive control (DeePC) paradigm to perform safe and optimal fast charging for lithium-ion batteries. The developed DeePC methodology is based on behavioral system theory and directly utilizes the input-output measurements from the battery system to predict the future trajectory and compute the optimal control policy. Constraints on input current and battery states are incorporated in the DeePC formulation to ensure battery fast charging with safe operations. Furthermore, we propose a principal component analysis based scheme to reduce the dimension of the optimization variables in the DeePC algorithm, which significantly enhances the computation efficiency without compromising the charging performance. Numerical simulations are performed on a high-fidelity battery simulator to validate the efficacy of the proposed fast charging strategy.

Keywords: Lithium-ion battery, fast charging, data-enabled predictive control, non-parametric model, model-free control

1. Introduction

Due to its zero-emission potential and high energy efficiency [1, 2, 3], lithium-ion (Li-ion) batteries have taken the forefront as the power source for electric vehicles (EVs). However, compared to gasoline-powered vehicles that can be fully refueled in minutes, the long charging time has been a major hurdle to the wider public adoption of Li-ion battery-powered EVs. Conventionally, the charging time of Li-ion battery can be reduced by increasing the charging current rate [4], which will, however, accelerate the battery degradation, shorten its lifespan, and bring potential safety hazards. Therefore, the development of fast charging technologies for Li-ion batteries needs not only to address the charging time but also to maintain the battery in a nondestructive charging mode for an extended lifespan.

Currently, constant-current constant-voltage (CC-CV) [5] charging is the most commonly used protocol for Li-ion batteries in industry. It consists of two charging phases: a *constant-current* phase in which the battery voltage is raised to a predetermined value, followed by a *constant-voltage* phase in which

the voltage remains constant until the current falls below a predetermined threshold. In addition, some variants, such as multistage constant current protocols [6, 7] and pulse charging protocols [8, 9], are designed to achieve faster charging and/or less battery degradation. However, it is empirically challenging and time-/cost- intensive to design and calibrate the appropriate charging profiles for these protocols. Moreover, they are unable to explicitly handle system constraints and not optimal with regard to metrics such as charging time, safety, and degradation.

To overcome the aforementioned difficulties, model-based optimization methods have been developed, where the commonly used battery models can be roughly grouped into equivalent circuit models (ECMs) and electrochemical models (EMs). ECMs integrate the models of different electrical components, including voltage source, resistors, and capacitors. With appropriate parameterization, the ECMs are able to characterize the electrical dynamics and some internal states of batteries, such as state-of-charge (SOC) [10, 11], terminal voltage [12], impedance [11], and heat generation [13]. Based on the established ECMs, the optimization techniques, such as dynamic programming [14], genetic algorithm [13, 15], fuzzy control [16], and min-max strategy [17], can be leveraged to generate optimal charging protocols for fast charging, while maintaining battery safety and mitigating degradation. However, ECMs can only mimic the external characteristics such as the voltage response of batteries and they are not able to model the electrochemical processes inside the cell, especially the side reactions

*The authors made equal contributions to this paper.

**Zhaojian Li is the corresponding author.

Email addresses: zhangk64@msu.edu (Kaixiang Zhang), chenkaia@msu.edu (Kaian Chen), lxflin@ucdavis.edu (Xinfan Lin), zhengyusheng@cqu.edu.cn (Yusheng Zheng), Xunyun.Yin@ntu.edu.sg (Xunyun Yin), xiaosonghu@ieee.org (Xiaosong Hu), ziyou@nus.edu.sg (Ziyou Song), lizhaoj1@msu.edu (Zhaojian Li)

triggered by fast charging. Therefore, charging protocols developed through ECMs will not be able to adequately suppress the side reactions due to the lack of explicit constraints on internal electrochemical states.

Conversely, the EMs [18] are developed based on first principles and can capture the internal mechanisms, e.g., ion diffusion and de-/intercalation in the electrodes and ion transport in the electrolyte. Hence, EMs can provide insights into electrochemical states of the battery. However, EMs are complex to establish and the model calibration is also a non-trivial task [4]. In addition, it is challenging to design suitable controllers based on such highly nonlinear and complex EMs. Attempts have been made to reduce EM complexity by the simplification of battery structure [19] and internal dynamics [20]. With the simplified models, many closed-loop optimal controls are formulated for battery fast charging. For instance, a fast charging protocol was developed in [21] based on a simplified EM, where the side reactions are controlled explicitly. By incorporating thermal dynamics into a similar EM, a reference governor based nonlinear model predictive control (MPC) [22] was proposed to reduce charging time and mitigate temperature-dependent degradation caused by lithium plating and the growth of solid electrolyte interphase. Although model-based approaches provide optimal solutions for fast charging in theory, robustness, and optimality can rarely be accomplished in practice because the Li-ion battery dynamics are constantly changing due to distinct operation modes and uncertainties.

The aforementioned observations, along with advancements in computing and sensing technology, have cultivated a trend toward model-free and data-driven control techniques. For example, reinforcement learning [23] and Neural Network-Based approximation [24] have been utilized to design optimal charging schemes for batteries. Although these techniques can use experimental data to learn a model or simulate uncertain behaviors, they require tedious tuning and training procedures and have limited interpretability. Recently, Data-Enabled Predictive Control (DeePC) emerged as a promising model-free optimal control paradigm that directly uses input-output data to achieve safe and optimal control of unknown systems [25]. In contrast to traditional model-based control schemes that rely on an accurate parametric model [26], DeePC leverages behavioral system theory [27] and Willems' fundamental lemma [28] to implicitly describe the system trajectories using collected input-output data [25]. It has been revealed that DeePC is equivalent to an MPC formulation for linear time-invariant (LTI) systems [29], and its application to nonlinear and stochastic systems shows promising performance with the aid of different regularization techniques [30, 31]. The DeePC is especially appealing to systems where the model is difficult or expensive to obtain, and it has been successfully implemented in different applications, including unmanned aerial vehicles [25], power grids [32], and connected and automated vehicles [33]. However, the high dimension of optimization variables in DeePC (usually higher than those in its MPC counterpart) makes it computationally expensive for real-time implementation. Therefore, it is crucial to develop effective methods to reduce the computational cost, enabling its application and

widespread adoption in actual engineering systems.

In this paper, we develop an efficient DeePC approach for fast charging of Li-ion batteries with constraint handling capabilities. Specifically, without relying on an explicit, complex battery model, an optimal charging controller is designed by utilizing measurable battery input and output data. Both input current and battery internal state constraints are explicitly considered in the DeePC formulation, ensuring a safe charging operation. Meanwhile, a novel principal component analysis (PCA) based scheme is developed to reduce the dimension of optimization variables and thus alleviate the computational burden of the control paradigm.

Our main contributions include the following. First, this paper spearheads the application of the DeePC framework to address the safe and fast charging of Li-ion batteries. The cumbersome modeling and validation processes of ECMs and EMs are circumvented by utilizing offline data collection and processing. Second, we develop a novel PCA-based dimension reduction method for the ease of DeePC online implementation, achieving much improved computation efficiency without degrading the system performance. Last but not least, the efficacy of the proposed scheme on fast charging of Li-ion batteries with safety related constraints is evaluated in a high-fidelity battery simulator. In comparison to the widely adopted CC-CV charging protocol and the conventional MPC method, the proposed scheme can achieve safer and more efficient charging.

The rest of this paper is organized as follows. Section 2 reviews the DeePC algorithm, as well as its regularized version. Section 3 introduces the DeePC algorithm for optimal charging of Li-ion battery systems. Section 4 presents the PCA-based dimension reduction method for the optimization variables of DeePC. Section 5 shows the simulation results, and conclusions are made in Section 6.

Nomenclature: We denote \mathbb{Z}_+ and \mathbb{R} as the set of positive integers and real numbers, respectively. 0 used in $[\cdot]$ is denoted as a zero vector with compatible size. The weighted 2-norm of a vector x is denoted by $\|x\|_P \triangleq \sqrt{x^\top P x}$, where $P \succ (\succcurlyeq) 0$ is a positive (semi-)definite matrix. Given a signal $\omega \in \mathbb{R}^n$ and two integers $i, j \in \mathbb{Z}_+$ with $i \leq j$, we denote by $\omega_{[i,j]}$ the restriction of ω to the interval $[i, j]$, namely, $\omega_{[i,j]} := [\omega^\top(i), \omega^\top(i+1), \dots, \omega^\top(j)]^\top$. To simplify notation, we will also use $\omega_{[i,j]}$ to denote the sequence $\{\omega(i), \dots, \omega(j)\}$. Given a matrix $A \in \mathbb{R}^{n \times m}$, we denote by $A_{[i,j]}$, $1 \leq i < j \leq m$ the restriction of A to the interval from i th column to j th column. We refer to $x(t)$ the system measurement at time instant t , while quantity x_{it} is a prediction value i time-steps ahead of current time instant t .

2. Preliminaries

2.1. Data-Enabled Predictive Control (DeePC)

DeePC was originally developed for LTI systems as a model-free optimal control strategy that does not rely on an explicit parametric model. Instead, it leverages Willems' fundamental lemma [28] and generates control inputs (and resultant system

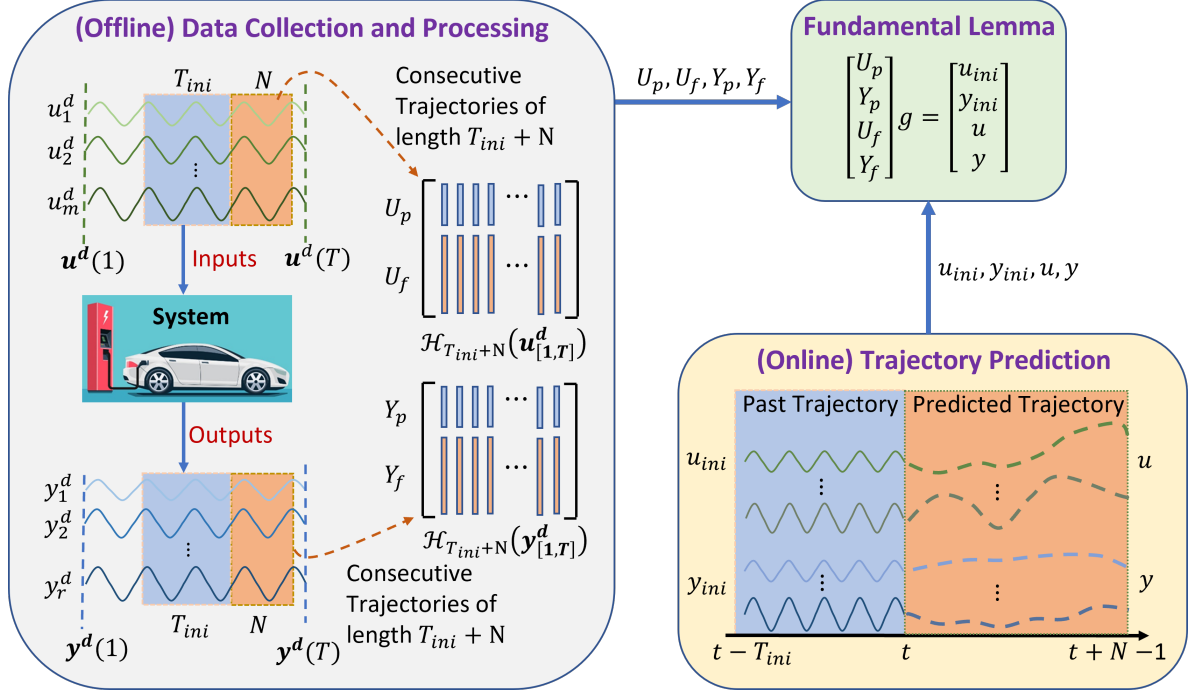


Figure 1: Schematic diagram of the data-enabled predictive control.

outputs) compatible with the pre-collected system data. Specifically, let $u^d = [u_1^d, u_2^d, \dots, u_m^d]^T \in \mathbb{R}^m$ be the control inputs and let $y^d = [y_1^d, y_2^d, \dots, y_r^d]^T \in \mathbb{R}^r$ be the system outputs. As shown in Figure 1, an input/output data sequence of length T is first collected, and the consecutive trajectories of length $T_{\text{ini}} + N$ are extracted to form the following Hankel matrices:

$$\mathcal{H}_L(u_{[1,T]}^d) = \begin{bmatrix} u^d(1) & u^d(2) & \dots & u^d(T-L+1) \\ u^d(2) & u^d(3) & \dots & u^d(T-L+2) \\ \vdots & \vdots & \ddots & \vdots \\ u^d(L) & u^d(L+1) & \dots & u^d(T) \end{bmatrix} = \begin{bmatrix} U_p \\ U_f \end{bmatrix},$$

$$\mathcal{H}_L(y_{[1,T]}^d) = \begin{bmatrix} y^d(1) & y^d(2) & \dots & y^d(T-L+1) \\ y^d(2) & y^d(3) & \dots & y^d(T-L+2) \\ \vdots & \vdots & \ddots & \vdots \\ y^d(L) & y^d(L+1) & \dots & y^d(T) \end{bmatrix} = \begin{bmatrix} Y_p \\ Y_f \end{bmatrix},$$

(1)

where $L = T_{\text{ini}} + N$, and U_p denotes the first T_{ini} block rows of $\mathcal{H}_L(u_{[1,T]}^d)$ and represents the “past” segment of the input trajectory whereas U_f denotes the last N block rows of $\mathcal{H}_L(u_{[1,T]}^d)$ and represents the “future” segment of the input trajectory. The matrices Y_p and Y_f are similarly defined. Essentially, the columns of $\mathcal{H}_L(u_{[1,T]}^d)$ and $\mathcal{H}_L(y_{[1,T]}^d)$ can be viewed as libraries of input/output trajectories of length L , which are further partitioned into segments with length T_{ini} (representing “past”) and length N (representing “future”) to be compatible with the online optimization formulation which will be discussed in later sections. We next introduce the following concept necessary for establishing our results.

Definition 2.1 (Persistently Exciting). *A signal sequence $w_{[1,T]}$*

is persistently exciting of order L ($L \leq T$) if the Hankel matrix $\mathcal{H}_L(w_{[1,T]})$ is of full row rank.

Remark 2.2 (Minimal Length of T [25]). *In order to make $w_{[1,T]}$ persistently exciting of order L , it must have $T \geq (m+1)L - 1$, that is, the input signal sequence $w_{[1,T]}$ should be sufficiently rich and long so as to fully excite the system yielding an output sequence that is representative for the system’s behavior.*

During the online implementation, at each time step t , an input/output trajectory of the past T_{ini} steps is buffered and used to form $u_{\text{ini}} = u_{[t-T_{\text{ini}}, t-1]}$ and $y_{\text{ini}} = y_{[t-T_{\text{ini}}, t-1]}$. Let $u = u_{[t, t+N-1]}$ and $y = y_{[t, t+N-1]}$ be the control inputs and the system outputs over the N -step prediction horizon, respectively. The Willems’ fundamental lemma states that if the pre-collected input sequence $u_{[1,T]}^d$ is persistently exciting of order $T_{\text{ini}} + N + n$ with n being the dimension of the system states (n can be chosen as an upper bound of state dimension [25]), then the patched trajectory $(u_{\text{ini}}, y_{\text{ini}}, u, y)$ is generated from the LTI system when it is spanned by (U_p, Y_p, U_f, Y_f) , that is, there exists a vector $g \in \mathbb{R}^{T-T_{\text{ini}}-N+1}$ such that:

$$\begin{bmatrix} U_p \\ Y_p \\ U_f \\ Y_f \end{bmatrix} g = \begin{bmatrix} u_{\text{ini}} \\ y_{\text{ini}} \\ u \\ y \end{bmatrix}, \quad (2)$$

which is a non-parametric system representation that ensures any consecutive trajectory of length $T_{\text{ini}} + N$ is compatible with those in the trajectory library in (1), and the initial trajectory $[u_{\text{ini}}^T, y_{\text{ini}}^T]^T$ can be viewed as setting an initial condition for the unknown future trajectory $[u^T, y^T]^T$. The DeePC can then be

cast as the following constrained optimization problem:

$$\begin{aligned} \min_{g,u,y} \quad & J(u, y) = \sum_{k=t}^{t+N-1} (\|y(k)\|_Q^2 + \|u(k)\|_R^2) \\ \text{s.t.} \quad & (2), \\ & y(k) \in \mathcal{Y}(k), \quad k = t, \dots, t + N - 1, \\ & u(k) \in \mathcal{U}(k), \quad k = t, \dots, t + N - 1, \end{aligned} \quad (3)$$

where $\mathcal{U}(k)$ and $\mathcal{Y}(k)$ represent the input and output constraints at time step k , respectively. As the DeePC bypasses the model identification step and directly optimizes the control from data, it has found great successes across various domains [25, 34, 32, 33].

2.2. Regularized DeePC

DeePC was first developed for deterministic LTI systems. For nonlinear systems, a regularization scheme has been developed to achieve satisfactory performance [25, 30, 35, 36]. In particular, for the input/output data collected from a nonlinear system, the subspace spanned by the constructed Hankel matrix may no longer be consistent with the subspace of trajectories from the underlying system, even if the Hankel matrix satisfies the full rank condition under such data sets collected from a nonlinear system. A direct consequence is that poor prediction performance is likely to happen with the ill-posed condition of Hankel matrix constraint. In this case, a penalty term is added for the discrepancy, quantified by a slack variable σ_y , between the estimated initial condition $Y_p g$ and the real-time buffered initial condition y_{ini} , which provides a least-square estimation of the true initial condition. Then with an additional regularization term, the corresponding regularized DeePC optimization problem is presented as:

$$\min_{g,u,y} J(u, y) + \lambda_y \|\sigma_y\|_2^2 + \lambda_g \|g\|_2^2 \quad (4a)$$

$$\text{s.t.} \quad \begin{bmatrix} U_p \\ Y_p \\ U_f \\ Y_f \end{bmatrix} g = \begin{bmatrix} u_{\text{ini}} \\ y_{\text{ini}} \\ u \\ y \end{bmatrix} + \begin{bmatrix} 0 \\ \sigma_y \\ 0 \\ 0 \end{bmatrix}, \quad (4b)$$

$$y(k) \in \mathcal{Y}(k), \quad k = t, \dots, t + N - 1, \quad (4c)$$

$$u(k) \in \mathcal{U}(k), \quad k = t, \dots, t + N - 1, \quad (4d)$$

where $\lambda_y, \lambda_g \in \mathbb{R}_+$ are the regularization parameters. This problem formulation (4) has been proved to coincide with a distributionally robust problem via the technique of Wasserstein metric [30, 35].

Remark 2.3 (selection of λ_y). λ_y can be chosen as a scalar to equally penalize the elements in $\sigma_y = Y_p g - y_{\text{ini}}$. Alternatively, λ_y can be designed as a penalty matrix to transform the second term in (4a) to be $\|\sigma_y\|_{\lambda_y}^2$, so that elements in σ_y can be penalized differently by assigning the weighting factor in the corresponding position of matrix λ_y .

3. DeePC for Li-ion Battery Fast Charging

In this section, we first briefly introduce the Li-ion battery system to provide background information on our considered application. Then, a non-parametric system representation is developed to characterize the charging dynamics directly based on input-output measurements, without the need for complicated battery models such as ECMs and EMs. Finally, we introduce the control objective and system constraints and present the full DeePC formulation for Li-ion battery charging.

3.1. Description of Li-ion Battery System

The working mechanism of Li-ion batteries is vastly complicated, with coupled chemical, electrical and thermal dynamics closely interacting with each other to influence the battery states. Physical or chemical reactions with different materials [37] take place at different regions inside the battery, leading to varying concentrations of lithium ions, including battery internal electrolyte concentration (c_e) and concentration inside or at the surface of solid material particles ($c_s^{\text{in}}/c_s^{\text{surf}}$), whose dependence on other battery states can be represented by the abstract partial differential equations:

$$\begin{aligned} \frac{\partial c_{e,i}(x, t)}{\partial t} + \mathcal{L}_1 c_{e,i}(x, t) &= F_1(I(t), c_{s,i}(x, t), T_{\text{emp}}(x, t), \eta_i), \\ \frac{\partial c_{s,i}(x, t)}{\partial t} + \mathcal{L}_2 c_{s,i}(x, t) &= F_2(I(t), c_{e,i}(x, t), T_{\text{emp}}(x, t), \eta_i), \end{aligned} \quad (5)$$

where \mathcal{L}_1 and \mathcal{L}_2 are operators acting on the abstract space of c_e and c_s for their spatial distributions. $F_1(\cdot)$ and $F_2(\cdot)$ are abstract nonlinear reaction functions that describe the intrinsic spatial-temporal relation of the lithium-ions inside the battery (see [18, 38] for the detailed forms). Here $i \in \mathcal{S}$ represents the index of the battery region, where $\mathcal{S} = \{\text{anode}, \text{separator}, \text{cathode}\}$. For detailed discussions about the battery region separation, interested readers can refer to [4]. I and T_{emp} represent the charging current and the battery temperature, respectively. Furthermore, η characterizes the over-potential of interface reactions and can be represented by [39, 40]:

$$\eta_i = \Phi_s(x, t) - \Phi_e(x, t) - U_i, \quad (6)$$

where Φ_e denotes the electrolyte potential on one side of the interface whereas Φ_s denotes the solid material potential on the other side; and U_i denotes the open circuit (or equilibrium) potential. The dependence of Φ_e and Φ_s on battery internal states can similarly be described in form of (5) as,

$$\begin{aligned} \frac{\partial \Phi_s(x, t)}{\partial t} + C_1 \Phi_s(x, t) &= G_1(I(t), c_{e,i}(x, t), c_{s,i}(x, t), T_{\text{emp}}(x, t)), \\ \frac{\partial \Phi_e(x, t)}{\partial t} + C_2 \Phi_e(x, t) &= G_2(I(t), c_{e,i}(x, t), c_{s,i}(x, t), T_{\text{emp}}(x, t)), \end{aligned} \quad (7)$$

where C_1 and C_2 are also the abstract operators, operating on Φ_s and Φ_e , respectively. $G_1(\cdot)$ and $G_2(\cdot)$ abstractly describe the battery internal relations among all states. The aforementioned function formats can generally take the form of partial differential-algebraic equations [18, 19, 20, 21, 22], which are

complex and tightly coupled. Furthermore, comprehensive Li-ion battery models also take into account the temperature variation driven by irreversible and reversible heat generations, with the following heat equation:

$$\frac{\partial T_{emp}(x, t)}{\partial t} + \mathcal{D}T_{emp}(x, t) = Q_{irr}(I(t)) + Q_{rev}(I(t)). \quad (8)$$

Here the operator \mathcal{D} characterizes the spatial gradient of the temperature in the battery; Q_{irr} represents the irreversible heat generation [41, 42, 43, 44], with resistive heating as a major source of contribution; and Q_{rev} represents the reversible heat process, also known as entropic heat [45].

In addition, boundary conditions in the above PDEs are required on the aforementioned battery states (e.g., $c_e, c_s, \Phi_e, \Phi_s, T_{emp}$) for a physically meaningful solution, i.e., all electrical and chemical reactions are limited within certain spatial regions of the battery and heat exchanges within the surrounding environment [4]. Furthermore, interface conditions [4, 40] are also required to enforce the continuity of the solution between two different materials inside the battery. It is obvious that the battery charging dynamics is very complicated and for control purposes, ECM and EM methods are typically reduced to a set of ordinary differential equations (ODEs),

$$\begin{aligned} \dot{z}(t) &= f(z(t), u(t)), \\ y(t) &= h(z(t), u(t)), \end{aligned} \quad (9)$$

where $f(\cdot)$ denotes the simplified model from (5) and (8), and $h(\cdot)$ is the output function. The system state z is chosen as a subset of the battery states (e.g., $c_e, c_s, \Phi_e, \Phi_s, T_{emp}$), and u is generally chosen as the charging current I . The control objective is to obtain an admissible control inputs $u(t) \in \mathcal{U}(t)$ such that when applied to system (9), the resulting output $y(t) \in \mathcal{Y}(t)$ is also admissible while minimizing a predefined cost function to achieve safe and fast battery charging. More formally, the optimization problem can be formulated as,

$$\begin{aligned} \min_{u, y} \quad & \int_t c(u(\tau), y(\tau)) d\tau \\ \text{s.t.} \quad & (9) \\ & u(t) \in \mathcal{U}(t), \quad y(t) \in \mathcal{Y}(t). \end{aligned} \quad (10)$$

Here $c(\cdot)$ denotes the running cost, starting from time instant t and integrated over a time period for the specified battery charging cycle. For example, several MPC frameworks have been proposed [22, 39, 46, 47]. However, it is clear from the above discussions that such model-based approaches are very challenging to design due to the exceedingly difficult modeling and calibration. Therefore, we next present an efficient data-enabled approach for effective controls by directly exploiting input-output data, without the need for the complex modeling process.

3.2. Non-Parametric Representation of Li-Ion Battery System for Fast charging

In this section, we present a non-parametric, data-driven system representation that directly describes the battery dynamics

using input-output data. Specifically, we exploit the behavioral system theory and Willems' fundamental lemma to characterize the system using the input-output data as detailed in Section II-B. More specifically, as shown in Figure 2, the system outputs are specified as battery voltage (y_V), battery temperature ($y_{T_{emp}}$), and state of charge (y_{soc}) while the system input is chosen as the charging current (I). Then an input-output trajectory of length T is collected by exciting the system with an input trajectory that is PE of order L . The inputs can be designed as sinusoidal signals or multi-level pseudo-random signals [48]. As a result, we obtain the following data vectors:

$$u_{[1, T]}^d = \begin{bmatrix} u^d(1) \\ \vdots \\ u^d(T) \end{bmatrix} \in \mathbb{R}^{mT}, \quad y_{[1, T]}^d = \begin{bmatrix} y^d(1) \\ \vdots \\ y^d(T) \end{bmatrix} \in \mathbb{R}^{rT},$$

with $u_{[1, T]}^d$ being the input charging current (I) sequence and $y_{[1, T]}^d$ the output sequence whose element $y(i) = [y_V(i), y_{T_{emp}}(i), y_{soc}(i)]^\top$, $i \in [1, T]$ consists of battery voltage (V), battery temperature (T_{emp}) and SOC. Note that even though SOC cannot be directly measured, reliable methods exist for accurate estimations [4]. Therefore, the choice of input-output data is practically viable. The pre-collected input-output data vector is then re-arranged into the Hankel matrices (1) for non-parametric representation of battery charging dynamics, with partitioned blocks corresponding to the ‘‘past’’ data of length T_{ini} and ‘‘future’’ data of length N .

Finally, during online implementation, $u_{ini} = u_{[t-T_{ini}, t-1]}$ and $y_{ini} = y_{[t-T_{ini}, t-1]}$ of length T_{ini} are buffered. Define $u = u_{[t, t+N-1]}$ and $y = y_{[t, t+N-1]}$ of length N as the control sequence and output sequence in the optimization horizon of length N , the system behavior can be represented by the non-parametric model (4b), which circumvents the major challenges in deriving and calibrating the complicated EMs and ECMs.

Remark 3.1 (Construction of Hankel matrix). *If it is challenging for the system to generate a long trajectory, e.g., the system has unstable dynamics or it is expensive to run a long test. In this case, multiple short system trajectories can be patched to construct the Hankel matrix, as long as it satisfies a collective persistency of excitation condition [49].*

3.3. DeePC Formulation for Li-ion Battery Fast Charging

The control goal here is to charge the Li-ion battery as fast as possible, while ensuring system safety. Specifically, the objective is to design an optimal charging current profile to complete the charging task with minimum time consumed, while satisfying safe working condition constraints. To facilitate the practical application, instead of using the total time as a cost during the whole charging process, the objective function is designed by driving SOC to a target value. In addition, to alleviate the current chattering phenomenon and maintain a smooth charging process, the input variation in successive optimization steps are penalized [39, 46, 50]. As a result, the cost function is designed as:

$$J(u, y) = \sum_{k=t}^{t+N-1} \left(\|y_{soc}(k) - r_{soc}\|_Q^2 + \|\Delta u(k)\|_R^2 \right), \quad (11)$$

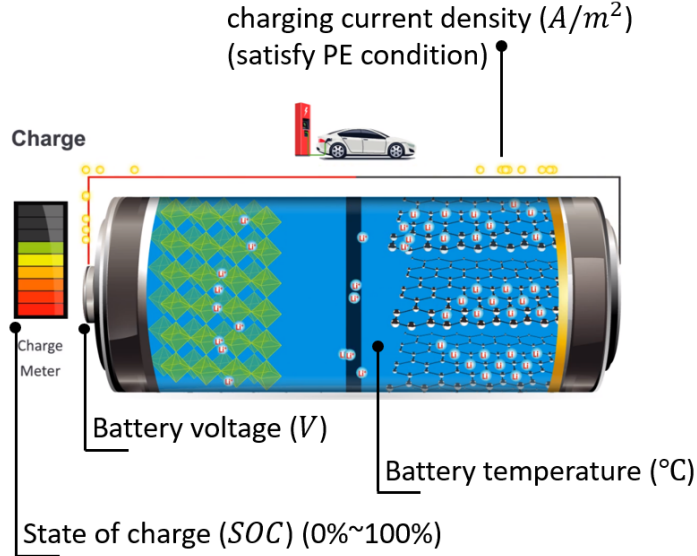


Figure 2: Measurable inputs and outputs of Li-ion batteries.

where Q and R are penalty matrices. By adding the regularization terms for DeePC extension to account for system nonlinearity, the cost function is reduced to the form of (4a).

To ensure safety during charging, in this paper, extreme charging scenarios are restricted: First, the charging rate will be maintained under $2C^1$, because rapid heat generation [21] is generally accompanied by high charging rate, causing battery degradation, and terminal voltage will also increase fast [39] to cut-off value, leading to an early termination of battery charging; Second, the limits of lower and upper cut-off voltages are considered, and if the limit is reached then the charging is stopped to avoid over-powered charging beyond safe charging zone [12]; and Third, the battery temperature is constrained between $25^\circ C$ and $31^\circ C$ to avoid accelerated battery degradation at high temperatures [21, 22, 51]. All these considerations are geared towards demonstrating the benefits of DeePC for Li-ion battery fast and safe charging purposes, without considering negligible battery internal side reactions. In the long run, however, the side reactions may cause irresistible degradation to the Li-ion battery, and lots of works are focusing on the avoidance and/or alleviation of such side reactions. Safe and fast charging of Li-ion battery with consideration of side reaction effects is still an open research field and will be considered in our future work.

To sum up, to maintain safe operations during charging, the following constraints are enforced:

$$\begin{aligned}
 I_{min} &\leq u(k) \leq I_{max}, \\
 \Delta I_{min} &\leq \Delta u(k) \leq \Delta I_{max}, \\
 V_{min} &\leq y_V(k) \leq V_{max}, \\
 T_{emp,min} &\leq y_{T_{emp}}(k) \leq T_{emp,max}, \\
 SOC_{init} &\leq y_{soc}(k) \leq SOC_{final},
 \end{aligned} \tag{12}$$

¹C-rate: it indicates the ratio of current magnitude to the battery size (battery nominal capacity).

where $I_{min/max}$ and $\Delta I_{min/max}$ denote the lower and upper bounds of input charging current and its fluctuation, respectively; $V_{min/max}$ denotes the cut-off voltage for low/high battery voltage bounds; $[T_{emp,min}, T_{emp,max}]$ denotes the desired battery working temperature range; and SOC_{init} and SOC_{final} are the desired starting point and ending point for battery charging, respectively. The specific values will be shown in Section 5.

4. DeePC with Dimension Reduction

Despite promising performance of (regularized) DeePC demonstrated in various applications, its computational complexity is high as it solves the optimization problem (4) with a large dimension of optimization variables $g \in \mathbb{R}^{T-T_{ini}-N+1}$, where T is often much larger than $T_{ini} + N$ to satisfy the persistent excitation (PE) condition. As a result, DeePC is generally more computationally expensive than its MPC counterpart. In this section, we exploit PCA [52] based method for dimension reduction to facilitate fast optimization while retaining the performance.

Specifically, we denote the left-side data matrix of (2) as A and the right-side data vector of (2) as b :

$$A := \begin{bmatrix} U_p \\ Y_p \\ U_f \\ Y_f \end{bmatrix}, \quad b := \begin{bmatrix} u_{ini} \\ y_{ini} \\ u \\ y \end{bmatrix}. \tag{13}$$

Note that in order to satisfy the PE condition and attain good performance, a large number of columns in A are generally used [25, 33]. Since the fundamental principle is that the columns of A must span the $T_{ini} + N$ continuous input/output trajectories, we employ PCA to identify the l most important representative trajectories, which we refer to as *eigen-trajectories*. Here l is a hyper-parameter that can be tuned. More specifically, the following dimension reduction steps are performed:

Table 1: Safety constraint values

I_{min}	ΔI_{min}	V_{min} [V]	T_{min} [°C]	SOC_{init} [%]
0	-0.1667C	2.1	25	5
I_{max}	ΔI_{max}	V_{max} [V]	T_{max} [°C]	SOC_{final} [%]
2C	0.1667C	4.17	31	95

- 1) Let $p = (m+r)(T_{ini}+N)$ and $q = T - T_{ini} - N + 1$, then the singular value decomposition (SVD) of matrix A is performed, as follows:

$$A = W\Sigma V^T, \quad (14)$$

where matrix $\Sigma \in \mathbb{R}^{p \times q}$ is a rectangular diagonal matrix and uniquely determined by A with all the singular values $\sigma_i = \Sigma_{ii}, i \leq \min\{p, q\}$ on the diagonal in descending order. The columns of matrix $W \in \mathbb{R}^{p \times p}$ and the columns of matrix $V \in \mathbb{R}^{q \times q}$ are called left-singular vectors and right-singular vectors of A , respectively. They also form two sets of orthogonal bases.

- 2) Choose the first l columns from V to form a new matrix which is denoted as $V_{[1:l]}$, where $l \leq q$. As the columns of V represent the principle mixture of system modes [53, C. 1] evolving in time, the first l columns of V are the corresponding most representative trajectories, which we call *eigen-trajectories*, and they are essentially utilized for mapping.
- 3) Define a new vector \bar{g} with the relationship to g as,

$$g = V_{[1:l]}\bar{g}, \quad (15)$$

where \bar{g} has the dimension l . The matrix $V_{[1:l]}$ here, as mentioned, is a mapping from \bar{g} to g .

- 4) The equation (2) in the DeePC problem can be replaced by

$$\bar{A}\bar{g} = b, \quad (16)$$

where $\bar{A} = W\Sigma V^T V_{[1:l]} = AV_{[1:l]}$, and the optimization variable changes from g to \bar{g} with a lower dimension. The same equation transformation and replacement can be applied to (4b).

Remark 4.1 (Selection of Column Length l). *Three methods can be used to choose l for truncation of right-singular matrix V to get $V_{[1:l]}$,*

- *Principal component spectrum analysis. Plot the main modes in descending order, l can be picked by identifying the 'elbow' point with the steepest slope or some other points with the required energy percentage along the curve.*
- *Cross-validation. it is a kind of trial-and-error method by evaluating a performance index defined based on the variation of the length l .*
- *Optimal Hard Threshold Method [54]. An optimal mode truncation point can be calculated by finding the underlying lower rank matrix, especially in cases under heavy noise corruption.*

5. Simulations

In this section, the DeePC approach for Li-ion battery fast charging problem with safety constraints is implemented via simulation to demonstrate its effectiveness. In addition, comparison is also made for the proposed PCA-based dimension

reduction strategy on DeePC, showing its advantages of promoting online optimization efficiency and, meanwhile, still retaining the optimal performance of DeePC without dimension reduction.

5.1. Experimental Setup

A high-fidelity battery simulation model - LIONSIMBA [40], is used as the plant for simulation studies. The LIONSIMBA simulator is built based on the first principles and can provide all battery dynamics related signals, so the aforementioned signals, i.e., battery voltage, temperature, SOC, and charging current, are measurable or estimated as those from a real Li-ion battery management system.

The offline data (u^d, y^d) is collected with the sampling interval chosen as $\Delta t = 10s$. Among this collected data set, the input data sequence u^d is designed as a combination of sinusoidal signals and multi-level pseudo-random signals for system excitation. The 'past' data length and 'future' data length are $T_{ini} = 60$ and $N = 70$, respectively. In the cost function of DeePC problem, only one of the three outputs (SOC) is penalized, with the corresponding weighting factor in $Q \in \mathbb{R}^{3 \times 3}$ selected as 10, and the weighting factor for charging current is chosen as $R = 0.1$. The coefficients of regularization terms are set as $\lambda_g = 10^5, \lambda_{y_{soc}, y_V} = 10^3$ and $\lambda_{y_T} = 10^6$. The lower and upper bounds for system constraints are listed in Table 1. Simulations are conducted using Matlab R2021b on Windows 10@3.6GHz PC with 8GB RAM. Before every simulation run, an ambient temperature $T_{amb} = 25^\circ C$ is set as the initial condition of the simulator, and the charging current is selected as $I = 0C$. Note that for the chemistry property of this simulator, 1C value is approximately $30A/m^2$.

5.2. Performance of DeePC for Li-ion Battery Fast Charging

In this simulation, a fast charging target is set to charge the Li-ion battery from 5% to 95% SOC, almost a full cycle charge of the Li-ion battery. Both the CC-CV charging protocol and an MPC method are also implemented to facilitate the comparison. Specifically, three CC-CV protocols are applied for Li-ion battery charging, where the pre-set cut-off voltage value is $V_{cutoff} = 4.15V$ and the constant charging currents are selected as 1.2C, 1.5C, and 2.0C, respectively. In CC-CV protocols, the battery is initially charged in CC mode until the battery voltage reaches the cut-off value, and then the remaining charging proceeds in CV mode until SOC reaches 95%. Moreover, for the MPC method, an auto-regressive with exogenous input (ARX) model is first estimated with the data set (u^d, y^d) (see Section 5.1 for more details about the data collection) to capture the battery charging dynamics, and then the MPC problem is formulated

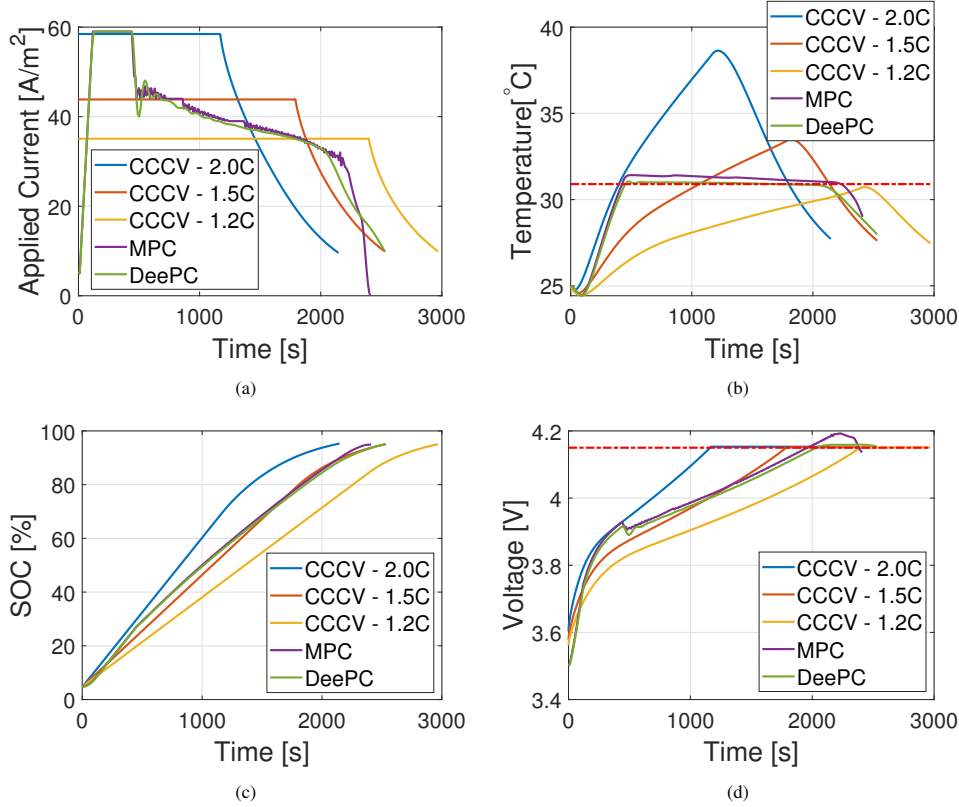


Figure 3: Simulation results of DeePC and CCCVs.

with the ARX model and the safety constraints considered in the DeePC scheme.

The simulation results are shown in Figure 3. As CC-CV cannot handle system constraints, constraint violations occur for CC-CV-1.5C and CC-CV-2.0C protocols as depicted in Figure 3b. The temperatures rise above the safe zone during battery charging, and it is hazardous to apply such charging protocols. To potentially overcome this problem, the CC-CV schemes are often conservatively designed at the sacrifice of charging speed. A typical example is the CC-CV-1.2C charging protocol, which is deliberately designed to satisfy all constraints. Nevertheless, the charging speed is the slowest, taking 2970 seconds to charge the SOC from 5% to 95%. Furthermore, it can be seen from Figures 3b and 3d that the MPC method oversteps the temperature and voltage constraints. As discussed in Section 3.1, the battery charging dynamics are highly nonlinear and complicated, making it difficult to identify a model that can fully reflect the system features. Because the performance of MPC is heavily reliant on the estimated model, the modeling error will result in performance degradation such as constraint violations.

In contrast, the DeePC is a data-driven optimal controller with the ability to deal with system constraints. As also shown in Figure 3, the DeePC not only satisfies all safety constraints, but also has a smoother charging current profile. DeePC's charging speed (2530 seconds) is nearly the same as CC-CV-1.5C (2531 seconds but it violates the constraints) and is approximately 15% faster than CC-CV-1.2C. In addition, to illustrate the prediction accuracy of DeePC for battery fast charging,

its prediction performances are compared with real system measurements at the same time instant. As shown in Figure 4a, the 1-step prediction performances of the three outputs match well with the system measurements. For the 10-step prediction case, shown in Figure 4b, even if certain deviations between successive prediction trajectories and the real measured ones exist, the overall trends of DeePC output prediction still have a good match to actual outputs. As a result, DeePC shows promising performance for Li-ion battery fast and safe charging while being simple and easy to implement.

5.3. Performance of DeePC with Dimension Reduction

The PCA-based dimension reduction method is applied to the aforementioned DeePC formulation, to demonstrate its ability of retaining optimal control performance while significantly reducing the computational complexity. Specifically, the Li-ion battery simulator is initialized under the conditions introduced in Section 5.1, and the control objective is to charge the SOC from 49% to 80%. According to the method detailed in Section 4, the matrix A is factorized with SVD, and a truncated right-singular matrix $V_{[1:l]}$ is chosen with $l = 700$ (the original total number of columns is $l_{max} = 1791$) to construct the matrix \tilde{A} . Figure 5 shows the performance comparison between the original DeePC and our PCA-based efficient DeePC. The close match of system input and outputs clearly demonstrates that the performance of the proposed efficient DeePC is as effective as that of the original DeePC. Moreover, the cost and computation time of these two methods are concluded in Table 2. The

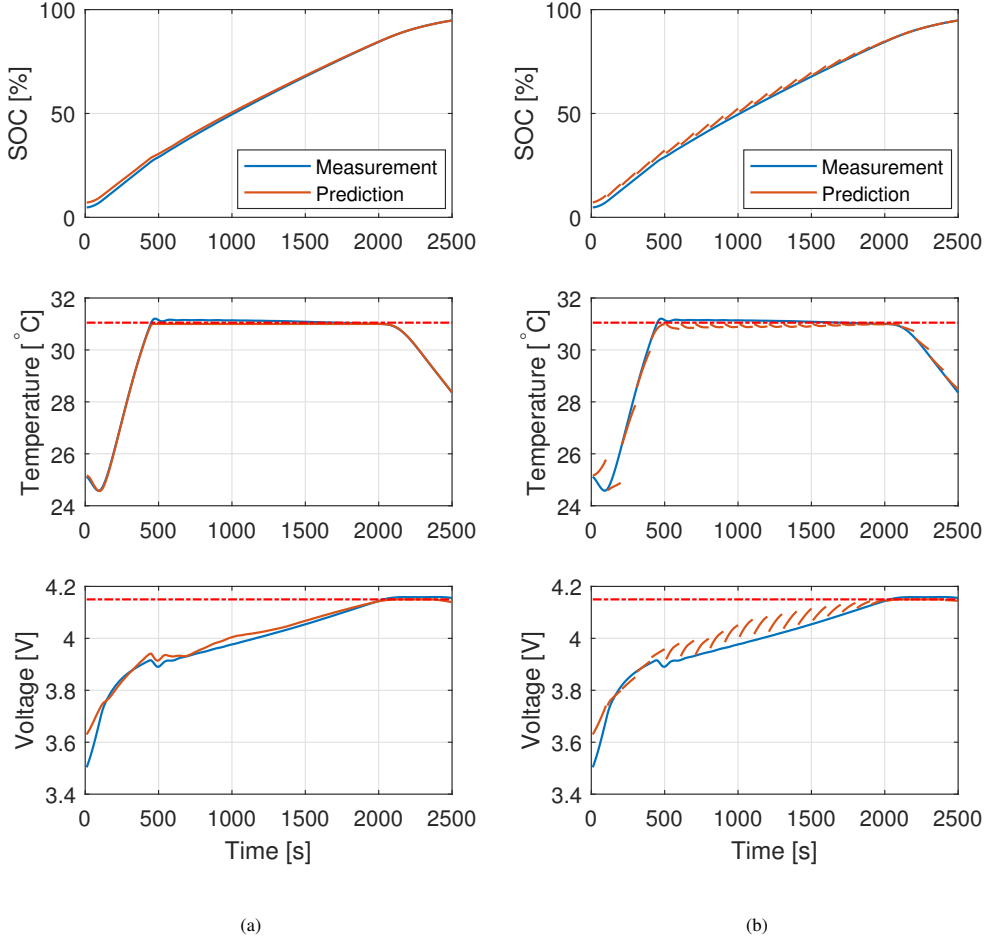


Figure 4: DeePC prediction and real system measurement. (a) Comparison between $y_{1|t}$ and $y(t+1)$, $t = 0, 1, 2, \dots$. (b) Comparison between $[y_{1|\bar{t}}, \dots, y_{10|\bar{t}}]$, $\bar{t} = 0, 10, 20, \dots$ and $y(t+1)$, $t = 0, 1, 2, \dots$.

Table 2: DeePC performance metrics based on A and \bar{A}

	$A \in \mathbb{R}^{520 \times 1791}$	$\bar{A} \in \mathbb{R}^{520 \times l}$ ($l = 700$)
Cost	261813.25	261813.26
Time per Step [sec]	2.2s	0.5s

costs of both DeePC methods are basically the same, while the time-per-step optimization of the proposed efficient DeePC is significantly less.

Further simulations are run by varying l to form matrices \bar{A} with different column numbers (i.e., different dimensions of the optimization variables). A comparison is conducted by directly truncating matrix A to make its size exactly the same as that of \bar{A} so that the computational resource used by these two cases are about the same to compare its control performance. The results are shown in Figure 6. It can be found that for $l \in [240, 1791]$, the cost function values of PCA-based DeePC can maintain stable and comparable performance within a large range. However, DeePC without PCA (i.e., direct truncation of matrix A) shows distinctly fluctuant cost values under different

l . Therefore, it is clear that the PCA-based dimension reduction strategy can significantly reduce the computational complexity while retaining the optimal performance comparable to the original DeePC scheme.

6. Conclusion

In this paper, we presented a novel DeePC approach for Li-ion battery fast charging with safety constraints. The DeePC approach only exploited input/output data for controller design, without the need for the complicated parametric battery model identification and calibration. In addition, to make DeePC online applicable with improved computational efficiency, a PCA-based dimension reduction approach was developed to significantly reduce computational time while retaining optimal system performance. Simulation results on a high-fidelity battery simulator confirmed the efficacy of the proposed scheme, with a 15% reduction in charging time as compared to the CC-CV-1.2C benchmark while satisfying all system constraints. Future work will include the integration of battery degradation metrics in the DeePC framework.

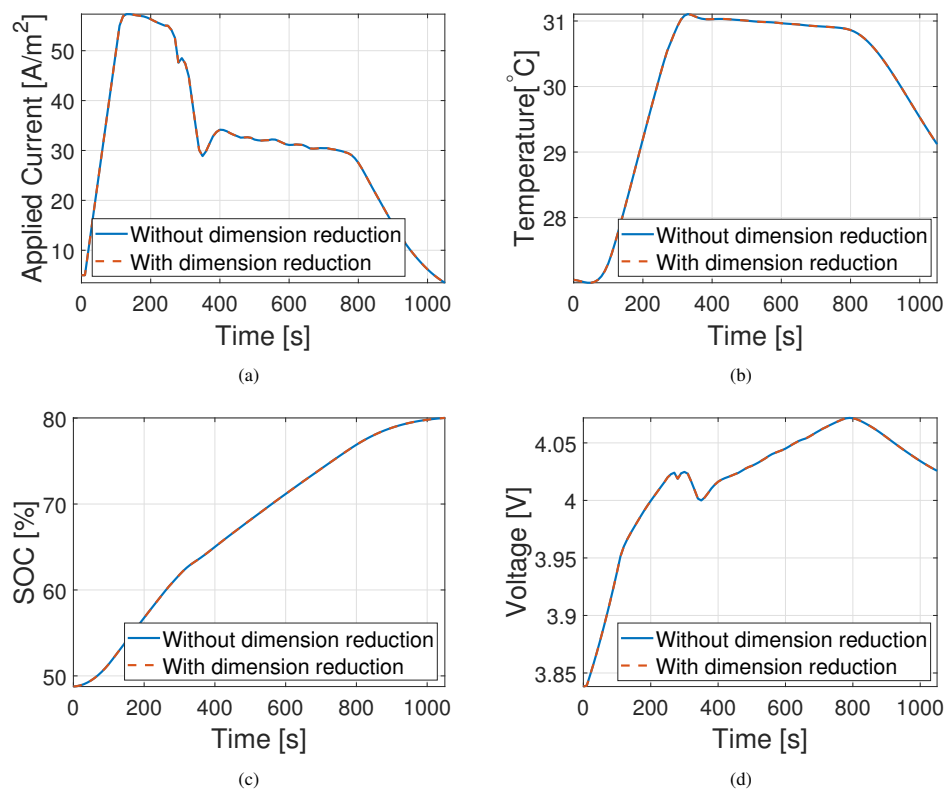


Figure 5: Simulation results of original DeePC and PCA-based DeePC

References

- [1] M. Armand, J.-M. Tarascon, Building better batteries, *Nature* 451 (7179) (2008) 652–657.
- [2] N. Wassiliadis, J. Schneider, A. Frank, L. Wildfeuer, X. Lin, A. Jossen, M. Lienkamp, Review of fast charging strategies for lithium-ion battery systems and their applicability for battery electric vehicles, *J. Energy Storage* 44 (2021) 103306.
- [3] W. Xie, X. Liu, R. He, Y. Li, X. Gao, X. Li, Z. Peng, S. Feng, X. Feng, S. Yang, Challenges and opportunities toward fast-charging of lithium-ion batteries, *J. Energy Storage* 32 (2020) 101837.
- [4] N. A. Chaturvedi, R. Klein, J. Christensen, J. Ahmed, A. Kojic, Algorithms for advanced battery-management systems, *IEEE Control Syst. Mag.* 30 (3) (2010) 49–68.
- [5] S. S. Zhang, K. Xu, T. Jow, Study of the charging process of a LiCoO₂-based li-ion battery, *J. Power Sources* 160 (2) (2006) 1349–1354.
- [6] S. S. Zhang, The effect of the charging protocol on the cycle life of a li-ion battery, *J. Power Sources* 161 (2) (2006) 1385–1391.
- [7] F. An, R. Zhang, Z. Wei, P. Li, Multi-stage constant-current charging protocol for a high-energy-density pouch cell based on a 622ncm/graphite system, *RSC Adv.* 9 (37) (2019) 21498–21506.
- [8] A. Aryanfar, D. Brooks, B. V. Merinov, W. A. Goddard III, A. J. Colussi, M. R. Hoffmann, Dynamics of lithium dendrite growth and inhibition: Pulse charging experiments and monte carlo calculations, *J. Phys. Chem. Lett.* 5 (10) (2014) 1721–1726.
- [9] J. Li, E. Murphy, J. Winnick, P. A. Kohl, The effects of pulse charging on cycling characteristics of commercial lithium-ion batteries, *J. Power Sources* 102 (1-2) (2001) 302–309.
- [10] T. T. Vo, X. Chen, W. Shen, A. Kapoor, New charging strategy for lithium-ion batteries based on the integration of taguchi method and state of charge estimation, *J. Power Sources* 273 (2015) 413–422.
- [11] H. Rahimi-Eichi, F. Baronti, M.-Y. Chow, Online adaptive parameter identification and state-of-charge coestimation for lithium-polymer battery cells, *IEEE Trans. Ind. Electron.* 61 (4) (2013) 2053–2061.
- [12] R. Drees, F. Lienesch, M. Kurrat, Fast charging lithium-ion battery formation based on simulations with an electrode equivalent circuit model, *J. Energy Storage* 36 (2021) 102345.
- [13] C. Zhang, J. Jiang, Y. Gao, W. Zhang, Q. Liu, X. Hu, Charging optimization in lithium-ion batteries based on temperature rise and charge time, *Appl. Energy* 194 (2017) 569–577.
- [14] Z. Chen, B. Xia, C. C. Mi, R. Xiong, Loss-minimization-based charging strategy for lithium-ion battery, *IEEE Trans. Ind. Appl.* 51 (5) (2015) 4121–4129.
- [15] Z. Guo, B. Y. Liaw, X. Qiu, L. Gao, C. Zhang, Optimal charging method for lithium ion batteries using a universal voltage protocol accommodating aging, *J. Power Sources* 274 (2015) 957–964.
- [16] S.-C. Wang, Y.-H. Liu, A pso-based fuzzy-controlled searching for the optimal charge pattern of li-ion batteries, *IEEE Trans. Ind. Electron.* 62 (5) (2014) 2983–2993.
- [17] Y. Parvini, A. Vahidi, Maximizing charging efficiency of lithium-ion and lead-acid batteries using optimal control theory, in: *Proc. Amer. Control Conf.*, 2015, pp. 317–322.
- [18] M. Doyle, T. F. Fuller, J. Newman, Modeling of galvanostatic charge and discharge of the lithium/polymer/insertion cell, *J. Electrochem. Soc.* 140 (6) (1993) 1526.
- [19] R. Klein, N. A. Chaturvedi, J. Christensen, J. Ahmed, R. Findeisen, A. Kojic, Optimal charging strategies in lithium-ion battery, in: *Proc. Amer. Control Conf.*, 2011, pp. 382–387.
- [20] R. Suresh, R. Rengaswamy, Modeling and control of battery systems. part ii: A model predictive controller for optimal charging, *Comput. Chem. Eng.* 119 (2018) 326–335.
- [21] Y. Yin, Y. Hu, S.-Y. Choe, H. Cho, W. T. Joe, New fast charging method of lithium-ion batteries based on a reduced order electrochemical model considering side reaction, *J. Power Sources* 423 (2019) 367–379.
- [22] Y. Yin, S.-Y. Choe, Actively temperature controlled health-aware fast charging method for lithium-ion battery using nonlinear model predictive control, *Appl. Energy* 271 (2020) 115232.
- [23] S. Park, A. Pozzi, M. Whitmeyer, H. Perez, A. Kandel, G. Kim, Y. Choi, W. T. Joe, D. M. Raimondo, S. Moura, A deep reinforcement learning framework for fast charging of li-ion batteries, *IEEE Trans. Transp. Elec-*

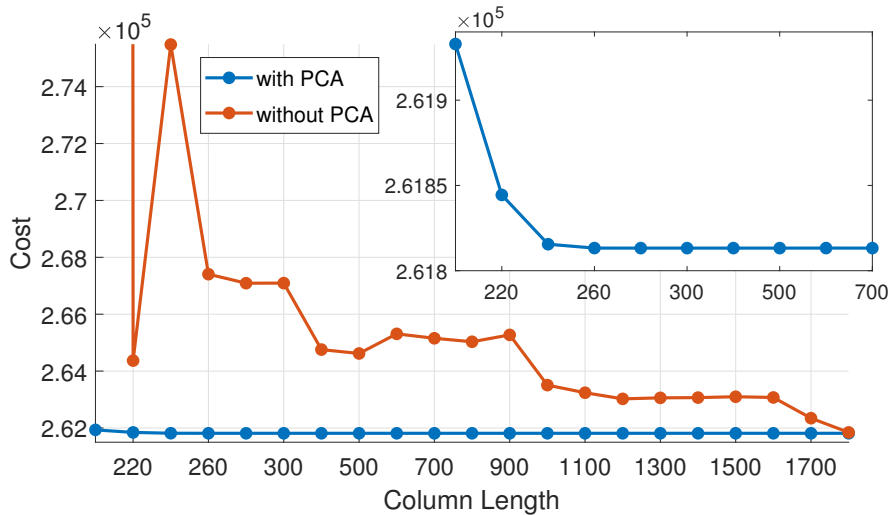


Figure 6: Cost comparison between the PCA-based DeePC and original DeePC in the case of same Hankel matrix size.

- trification 8 (2) (2022) 2770–2784.
- [24] A. Pozzi, S. Moura, D. Toti, A neural network-based approximation of model predictive control for a lithium-ion battery with electro-thermal dynamics, in: Proc. IEEE Int. Conf. Control & Autom., 2022, pp. 160–165.
- [25] J. Coulson, J. Lygeros, F. Dörfler, Data-enabled predictive control: In the shallows of the DeePC, in: Proc. Eur. Control Conf., 2019, pp. 307–312.
- [26] J. Rawlings, D. Mayne, M. Diehl, Model Predictive Control: Theory, Computation, and Design, Nob Hill Publishing, 2017.
- [27] I. Markovsky, J. C. Willems, S. Van Huffel, B. De Moor, Exact and Approximate Modeling of Linear Systems, Society for Industrial and Applied Mathematics, 2006.
- [28] J. C. Willems, P. Rapisarda, I. Markovsky, B. L. De Moor, A note on persistency of excitation, Syst. Control Lett. 54 (4) (2005) 325–329.
- [29] F. Fiedler, S. Lucia, On the relationship between data-enabled predictive control and subspace predictive control, in: Proc. Eur. Control Conf., 2021, pp. 222–229.
- [30] J. Coulson, J. Lygeros, F. Dörfler, Regularized and distributionally robust data-enabled predictive control, in: Proc. IEEE Conf. Decis. Control, 2019, pp. 2696–2701.
- [31] F. Dörfler, J. Coulson, I. Markovsky, Bridging direct and indirect data-driven control formulations via regularizations and relaxations, IEEE Trans. Autom. Control (2022) 1–1.
- [32] L. Huang, J. Coulson, J. Lygeros, F. Dörfler, Decentralized data-enabled predictive control for power system oscillation damping, IEEE Trans. Control Syst. Technol. 30 (3) (2022) 1065–1077.
- [33] J. Wang, Y. Zheng, Q. Xu, K. Li, Data-driven predictive control for connected and autonomous vehicles in mixed traffic, in: Proc. Amer. Control Conf., 2022, pp. 4739–4745.
- [34] P. G. Carlet, A. Favato, S. Bolognani, F. Dörfler, Data-driven continuous-set predictive current control for synchronous motor drives, IEEE Trans. Power Electron. 37 (6) (2022) 6637–6646.
- [35] J. Coulson, J. Lygeros, F. Dörfler, Distributionally robust chance constrained data-enabled predictive control, IEEE Trans. Autom. Control 67 (7) (2022) 3289–3304.
- [36] E. Elokda, J. Coulson, P. N. Beuchat, J. Lygeros, F. Dörfler, Data-enabled predictive control for quadcopters, Int. J. Robust Nonlinear Control 31 (18) (2021) 8916–8936.
- [37] N. Nitta, F. Wu, J. T. Lee, G. Yushin, Li-ion battery materials: present and future, Mater. Today 18 (5) (2015) 252–264.
- [38] C. D. Rahn, C.-Y. Wang, Battery systems engineering, John Wiley & Sons, 2013.
- [39] C. Zou, X. Hu, Z. Wei, T. Wik, B. Egardt, Electrochemical estimation and control for lithium-ion battery health-aware fast charging, IEEE Trans. Ind. Electron. 65 (8) (2017) 6635–6645.
- [40] M. Torchio, L. Magni, R. B. Gopaluni, R. D. Braatz, D. M. Raimondo, Lionsimba: a matlab framework based on a finite volume model suitable for li-ion battery design, simulation, and control, J. Electrochem. Soc. 163 (7) (2016) A1192.
- [41] C. Heubner, M. Schneider, C. Lämmel, A. Michaelis, Local heat generation in a single stack lithium ion battery cell, Electrochim. Acta 186 (2015) 404–412.
- [42] D. Danilov, P. Notten, Mathematical modelling of ionic transport in the electrolyte of li-ion batteries, Electrochim. Acta 53 (17) (2008) 5569–5578.
- [43] D. Grazioli, M. Magri, A. Salvadori, Computational modeling of li-ion batteries, Comput. Mech. 58 (6) (2016) 889–909.
- [44] D. Andre, M. Meiler, K. Steiner, C. Wimmer, T. Soczka-Guth, D. Sauer, Characterization of high-power lithium-ion batteries by electrochemical impedance spectroscopy. i. experimental investigation, J. Power Sources 196 (12) (2011) 5334–5341.
- [45] K. Jalkanen, T. Aho, K. Vuorilehto, Entropy change effects on the thermal behavior of a lifepo4/graphite lithium-ion cell at different states of charge, J. Power Sources 243 (2013) 354–360.
- [46] M. Torchio, N. A. Wolff, D. M. Raimondo, L. Magni, U. Krewer, R. B. Gopaluni, J. A. Paulson, R. D. Braatz, Real-time model predictive control for the optimal charging of a lithium-ion battery, in: Proc. Amer. Control Conf., 2015, pp. 4536–4541.
- [47] Y. Lu, X. Han, G. Zhao, L. Lu, M. Ouyang, Optimal charging of lithium-ion batteries based on model predictive control considering lithium plating and cell temperature, in: Proc. Int. Conf. Power Renew. Energy, 2021, pp. 1248–1253.
- [48] M. Braun, D. Rivera, A. Stenman, W. Foslien, C. Hrenya, Multi-level pseudo-random signal design and “model-on-demand” estimation applied to nonlinear identification of a RTP wafer reactor, in: Proc. Amer. Control Conf., 1999, pp. 1573–1577.
- [49] H. J. van Waarde, C. De Persis, M. K. Camlibel, P. Tesi, Willems’ fundamental lemma for state-space systems and its extension to multiple datasets, IEEE Control Syst. Lett. 4 (3) (2020) 602–607.
- [50] N. Tian, H. Fang, Y. Wang, Real-time optimal lithium-ion battery charging based on explicit model predictive control, IEEE Trans. Ind. Informat. 17 (2) (2020) 1318–1330.
- [51] T. C. Bach, S. F. Schuster, E. Fleder, J. Müller, M. J. Brand, H. Lorrmann, A. Jossen, G. Sextl, Nonlinear aging of cylindrical lithium-ion cells linked to heterogeneous compression, J. Energy Storage 5 (2016) 212–223.
- [52] M. E. Wall, A. Rechtsteiner, L. M. Rocha, Singular value decomposition and principal component analysis, in: A practical approach to microarray data analysis, Springer, 2003, pp. 91–109.
- [53] S. L. Brunton, J. N. Kutz, Data-driven science and engineering: Machine learning, dynamical systems, and control, Cambridge University Press, 2022.
- [54] M. Gavish, D. L. Donoho, The optimal hard threshold for singular values is $4/\sqrt{3}$, IEEE Trans. Inf. Theory 60 (8) (2014) 5040–5053.